MICROBIOLOGY

RESEARCH ARTICLE

Sheehan *et al.*, *Microbiology* 2019;165:863–875

DOI 10.1099/mic.0.000813

MICROBIOLOGY SOCIETY

Utilization of *Galleria mellonella* larvae to characterize the development of *Staphylococcus aureus* infection

Gerard Sheehan, Amy Dixon and Kevin Kavanagh*

Abstract

Staphylococcus aureus is a human opportunistic pathogen that causes a wide range of superficial and systemic infections in susceptible patients. Here we describe how an inoculum of *S. aureus* activates the cellular and humoral response of *Galleria mellonella* larvae while growing and disseminating throughout the host, forming nodules and ultimately killing the host. An inoculum of *S. aureus* (2×10^6 larva^{-1}) decreased larval viability at 24 (80±5.77%), 48 (55.93±5.55%) and 72 h (10.23±2.97%) and was accompanied by significant proliferation and dissemination of *S. aureus* between 6 and 48 h and the formation of nodules in the host. The hemocyte (immune cell) densities increased between 4 and 24 h and hemocytes isolated from larvae after 24 h exposure to heat-killed *S. aureus* (2×10^6 larva^{-1}) showed altered killing kinetics as compared to those from control larvae. Alterations in the humoral immune response of larvae 6 and 24 h post-infection were also determined by quantitative shotgun proteomics. The proteome of 6 h-infected larvae was enriched for antimicrobial proteins, proteins of the prophenoloxidase cascade and a range of peptidoglycan recognition proteins. By 24 h there was a significant increase in the abundance of a range of antimicrobial peptides with anti-staphylococcal activity and proteins associated with nodule formation. The results presented here indicate how *S. aureus* interacts with the larval immune response, induces the expression of a variety of immune-related peptides and also forms nodules which are a hallmark of soft tissue infections during human infection.

INTRODUCTION

Staphylococcus aureus is a facultative anaerobic, Gram-positive bacterium that colonizes approximately 30 % of the world's population on a range of body sites. *Staphylococcus* is the most frequent cause of biofilm/medical device-related infections [1], most likely due to being a body commensal. The most frequent sites of *S. aureus* colonization are the nose, skin and gastrointestinal (GI) tract [2]. *S. aureus* colonization is mostly non-symptomatic, but in the correct situation it is capable of causing a wide variety of diseases, from furuncles and boils to serious infections such as pneumonia, toxic shock syndrome and endocarditis [3].

The virulence of *S. aureus* is multifaceted and comes from an arsenal of effectors which enable interactions with the host, immune cell evasion and the induction of tissue damage [4]. *S. aureus* 33 kDa protein alpha toxin can induce pro-inflammatory conditions and pore formation in mammalian cells, resulting in necrosis. It has been suggested that alpha toxin creates an enhanced infection microenvironment for disease progression [5]. A range of superantigens are able to induce inflammation, which can result in toxic shock syndrome and sepsis by non-specific activation of T-cell proliferation through interactions with MHC class II molecules on antigen presentation cells [6]. *S. aureus* can inhibit the mammalian complement pathway via chemotaxis inhibitory protein of staphylococci binding of the C5a receptor and staphylococcal complement inhibitor blocking of C3 convertase activity [7, 8]. Coagulase and von Willebrand factor binding protein activate fibrin clot formation, facilitating the formation of staphylococcal aggregates in the blood, and this is mediated by clumping factors A and B [9, 10]. Fibronectin-binding proteins A and B (FnBPA/B) bind to integrin $\alpha5\beta1$, enabling the tethering of *S. aureus* to endothelial cells and phagocytic cells during infection [11].

Many experimental *in vivo* systems to characterize *S. aureus* infection dynamics have been developed, including cutaneous [12], renal [13] sepsis in mice [14] and endocarditis

Received 20 February 2019; Accepted 28 April 2019; Published 20 May 2019
Author affiliations: [1]Department of Biology, Maynooth University, Maynooth, Co. Kildare, Ireland.
***Correspondence:** Kevin Kavanagh, Kevin.Kavanagh@mu.ie
Keywords: *Galleria*; infection; immunity; mini-model; *Staphylococcus*.
Abbreviations: AMP, antimicrobial peptide; DEP, differentially expressed protein (DEP); FDR, false discovery rate; GO, gene ontology; SSDA, statistically significant differentially abundant.
Three supplementary figures are available with the online version of this article.

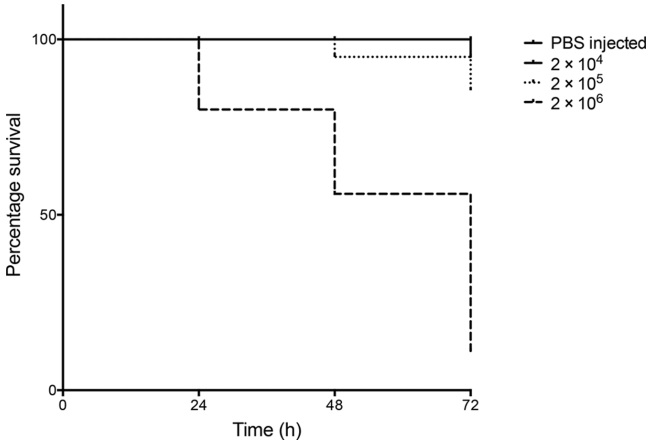

Fig. 1. Effect of *S. aureus* cells on viability of *G. mellonella* larvae over 72 h. *G. mellonella* larvae were inoculated with 20 µl *S. aureus* at doses ranging from 2×10^4 to 2×10^6 and incubated at 37 °C, and then viability was assessed over 72 h.

in rats [15]. Alternative systems are also used and include models to study bloodstream infection and pathogenesis using zebrafish [16] and digestive tract infection in *Caenorhabditis elegans* [17]. Insects are now widely employed to study different aspects of microbial pathogenesis [18–20]. The immune system of insects shares many similarities with the innate immune response of mammals and as a consequence insects may be used to assess the virulence of microbial pathogens and produce results comparable to those obtained using mammalian systems [21–23]. Larvae of *Galleria mellonella* (the greater wax moth) can be used to assess the virulence of fungal or bacterial pathogens, measure the *in vivo* toxicity of compounds and determine the *in vivo* activity of antimicrobial drugs [24–26]. *G. mellonella* larvae have many advantages as an *in vivo* model, as they are easy to inoculate, are free from legal and ethical restrictions, produce results in a short space of time, are amenable to incubation at 37 °C and, due to advances in 'omic' technologies, are now utilized to characterize the immune response to a variety of pathogens [24, 25]. *G. mellonella* larvae have used to study the virulence of Gram-positive bacteria such as *Streptococcus pyogenes* [27], *Streptococcus pneumoniae* [28], *Enterococus faecalis* [29, 30], *Enterococcus faecium* [31, 32], *Staphylococcus aureus* [33, 34] and *Listeria monocytogenes* [35, 36], and Gram-negative bacteria such as *Pseudomonas aeruginosa* [37, 38], *Escherichia coli* [39, 40], *Klebsiella pneumoniae* [41, 42], *Legionella pneumophila* [43, 44] and *Acinetobacter baumanii* [45, 46]. The aim of the work presented here was to examine the interaction of *S. aureus* with the larval immune

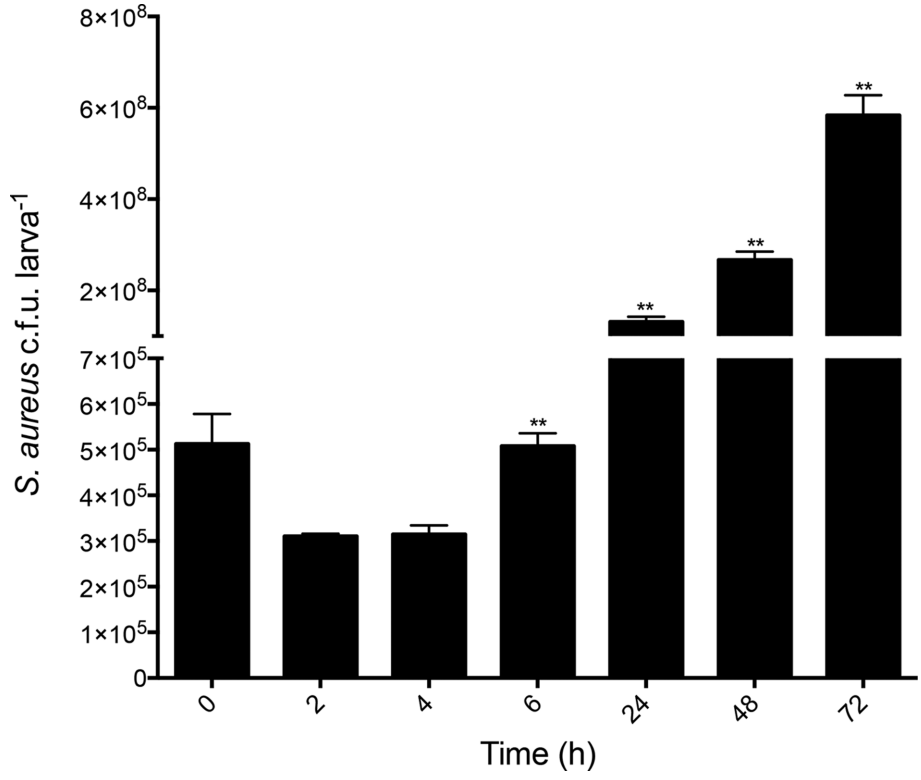

Fig. 2. *S. aureus* c.f.u. per larva obtained from *G. mellonella* larvae infected with *S. aureus* cells (2×10^6 larva^{-1}) over 72 h. Infection with *S. aureus* resulted in an increase in bacterial load in larvae from 6 until 72 h, as determined by plating on nutrient agar plates. Statistical analysis was carried out by comparing each time point to the previous time point (*P<0.05, **P<0.01). All values are the mean ±SE of three independent experiments.

response and to characterize similarities with the mammalian response in order to better establish this system as a model for studying *S. aureus* infection processes.

METHODS

Larval culture and inoculation

Sixth instar larvae of the greater wax moth *G. mellonella* (Livefoods Direct Ltd, UK) were stored in the dark at 15 °C and maintained on wood chippings as previously reported [19, 23]. Larvae weighing 0.22±0.03 g were selected and used within 2 weeks of receipt. Ten healthy larvae per treatment and controls were placed in sterile 9 cm Petri dishes lined with Whatman filter paper and containing some wood shavings. Larvae were inoculated with *S. aureus* through the last left pro-leg into the hemocoel with a Myjector U-100 insulin syringe (Terumo Europe N.V., Belgium). Larvae were acclimatized to 37 °C for 1 h prior to all experiments and incubated at 37 °C for all studies. All experiments were performed independently on three separate occasions.

S. aureus strains and culture conditions

S. aureus (clinical isolate) and green fluorescent protein (GFP)-tagged *S. aureus* strain SH1000 (a kind gift from Professor Joan Geoghegan, Trinity College Dublin, Ireland) were transferred aseptically using a sterile loop from a single colony grown on nutrient agar to nutrient broth (Oxoid) and grown overnight at 37 °C and 200 r.p.m. to the early stationary phase as previously described [47]. Cells were harvested by centrifugation (5000 ***g***) and cell pellets were washed three times with phosphate-buffered saline (PBS) prior to injection into larvae. Stocks were maintained on nutrient agar plates.

Determination of proliferation of *S. aureus* in *G. mellonella* larvae

An inoculum of 2×10^6 *S. aureus* cells $larva^{-1}$ was achieved by inoculating larvae with 20 µl of a 0.01 OD_{600} suspension of *S. aureus* in PBS solution. Infected larvae (n=3) were homogenized in a pestle and mortar with 3 ml of PBS, serially diluted (10^{-4} and 10^{-5}), plated onto nutrient agar plates and incubated at 37 °C for 24 h. The bacterial load was calculated as the number of *S. aureus* colony-forming units (c.f.u.) per larva and was based on the number of colonies that grew at specific dilutions. Samples of bacteria were plated onto CHROMagar plates to confirm their identity as *S. aureus*. Previous workers used selective media in this assay format [48], but a selective medium was not used here, as it was established that serial dilution of samples from uninfected larvae to the same levels as infected samples did not result in any indigenous bacteria growing on plates.

Cryo-imaging of *S. aureus* infection in *G. mellonella*

G. mellonella were inoculated with 2×10^6 *S. aureus* cells $larva^{-1}$ and incubated for 0, 6 and 24 h. Larvae (n=3) were embedded in Cryo-Imaging Embedding Compound (Bioinvision), flash-frozen in liquid nitrogen and mounted on a stage for sectioning according to the method described in [18]. Sectioning and imaging was carried out every 10 µm using a Cryoviz (Bioinvision, Inc., OH, USA) cryo-imaging system.

Confocal imaging of bacterial nodules

G. mellonella larvae (n=3) infected with *S. aureus* wild-type (WT) and GFP-labelled *S. aureus* (2×10^6 $larva^{-1}$) for 6 and 24 h were dissected in PBS and nodules were dissected apart with fine needles and transferred to a glass slide. The cells were washed twice (PBS) and a cover slide was placed on top. The cover slides were fixed *in situ* by applying a clear sealing solution around the perimeter of the slide, which also prevented the sample drying out. Cells were viewed with an Olympus Fluoview 1000 confocal microscope.

Determination of hemocyte density

The larval hemocyte density was determined as described in [18, 19] by inoculation of viable *S. aureus* (2×10^6 $larva^{-1}$). Changes in hemocyte density were assessed by bleeding 40 µl from each *G. mellonella* larva (n=5) into a micro-centrifuge tube on ice to prevent melanization. Hemolymph was diluted in 0.37 % (v/v) mercaptoethanol-supplemented PBS and cell density was determined using a hemocytometer. Hemocyte density was expressed in terms of hemocyte density/larva. Experiments were performed on three independent occasions and the means±standard error (SE) were determined.

Determination of microbicidal activity of hemocytes

Larvae were treated with heat-killed (95 °C, 15 min) *S. aureus* (2×10^6 $larva^{-1}$) and hemocytes extracted 6 and 24 h post-inoculation. Hemocytes were mixed with pre-opsonized *Candida albicans* cells at a ratio of 2 : 1 in a thermally controlled stirring chamber at 37 °C. Aliquots were taken at t=0, 20, 40, 60 and 80 min and plated on YEPD (Yeast extract, peptone, dextrose) agar plates supplemented with erythromycin (1 % w/v) as described in [18, 19].

Label-free quantitative (LFQ) proteomics of larval hemolymph

Label-free shotgun quantitative proteomics was conducted on hemocyte-free hemolymph from larvae (n=10) at 0, 6 and 24 h post-infection with *S. aureus* (2×10^6 $larva^{-1}$). Protein (75 µg) was prepared according to established protocols [19]. Protein identification from the tandem mass spectometry (MS/MS) data was performed using the Andromeda search engine in MaxQuant (version 1.2.2.5; http://maxquant.org/) to correlate the data against a six-frame translation of the expressed sequence tag (EST) contigs for *G. mellonella* [49, 50].

Results processing, statistical analyses and graphics generation were conducted using Perseus v. 1.5.5.3. LFQ intensities were $\log_2$-transformed and analysis of variance (ANOVA) of significance and t-tests between the hemolymph proteomes of 0, 6 and 24 h *S. aureus*-treated larvae were performed using a P value of 0.05 and significance was determined using false discovery rate (FDR) correction (Benjamini–Hochberg). Proteins that had non-existent values (indicative of absence or very low abundance in a sample) were also used in

statistical analysis of the total differentially expressed group following imputation of the zero values using a number close to the lowest value of the range of proteins plus or minus the standard deviation. After data imputation these proteins were included in subsequent statistical analysis.

Statistical analysis

All experiments were performed on three independent occasions and the results are expressed as the mean±SE. All statistical analysis was performed using GraphPad Prism v. 6.00 (one-way ANOVA analysis for hemocyte density and c.f.u. analysis and two-way ANOVA for hemocyte activity assay). Differences were considered significant at $P<0.05$.

Data availability

The MS proteomics data and MaxQuant search output files have been deposited at the ProteomeXchange Consortium [51] via the PRIDE partner repository with the dataset identifier PXD012766.

RESULTS

Response of *G. mellonella* larvae to *S. aureus* infection

Larvae were inoculated with an inoculum of *S. aureus* (2×10^4–2×10^6 cells larva^{-1}) and incubated at 37 °C, and then viability was assessed over 72 h. An inoculum of 2×10^4 cells larva^{-1} resulted in no change in larval viability over 72 h. An inoculum of 2×10^5 cells larva^{-1} resulted in no change in larval viability over 24 h, but at 48 and 72 h viability was reduced to 96.66±3.33 % and 84.43±2.94 %, respectively. An inoculum of 2×10^6 cells larva^{-1} resulted in the largest decrease in larval viability at 24 (80±5.77 %), 48 (55.93±5.55 %) and 72 h (10.23±2.97 %) as compared to the control (Fig. 1).

Between 4 and 6 h post-infection, *S. aureus* c.f.u. larva^{-1} increased from $3.14\pm0.19\times10^5$ to $5.08\pm0.28\times10^5$ ($P<0.01$). There was also an increase in *S. aureus* c.f.u. larva^{-1} at 24 ($1.31\pm0.11\times10^8$, $P<0.01$), 48 ($2.76\pm0.18\times10^8$, $P<0.01$) and 72 h ($5.83\pm0.44\times10^8$, $P<0.01$) (Fig. 2).

Dissemination of *S. aureus* infection through larvae

Cryo-imaging was employed to visualize the stages of invasion and dissemination of *S. aureus* through *G. mellonella* larvae. Larvae were inoculated with viable *S. aureus* (2×10^6 20 µl^{-1}) as described (white arrows). Small discrete nodules appeared around the perimeter of the haemocoel 6 h post-infection (black arrows), indicating the dissemination of *S. aureus* from the site of infection. By 24 and 48 h there was extensive melanization (red arrows) of larval tissue. The formation of large nodules at the site of inoculation was also apparent at 24 and 48 h post-infection (Fig. 3).

Confocal microscopy was employed at 6, 24 and 48 h post-infection and revealed the presence of GFP-labelled viable *S. aureus* (blue arrows) within nodules formed during infection. Interestingly, at 6 h, cells were clumped together during the nodulation process (Fig. 4). WT *S. aureus* without GFP produced no fluorescence and was included as a control for auto-fluorescence (Fig. S1, available in the online version of this article).

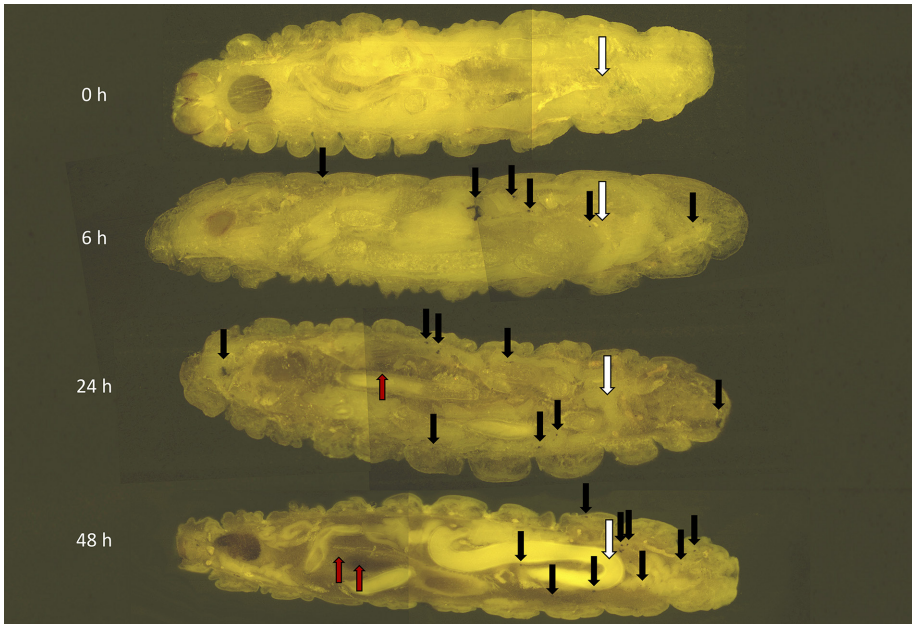

Fig. 3. Cryoviz visualization of disseminated *S. aureus* infection of *G. mellonella* larvae at 6, 24 and 48 h. Larvae were inoculated with 2×10^6 viable *S. aureus* cells for 6, 24 and 48 h and embedded, sectioned (10 µm) and visualized using a Cryoviz (Bioinvision, Inc., OH, USA) cryo-imaging system. White arrows, point of inoculation; black arrows, bacterial nodules; red arrows, extensive melanization.

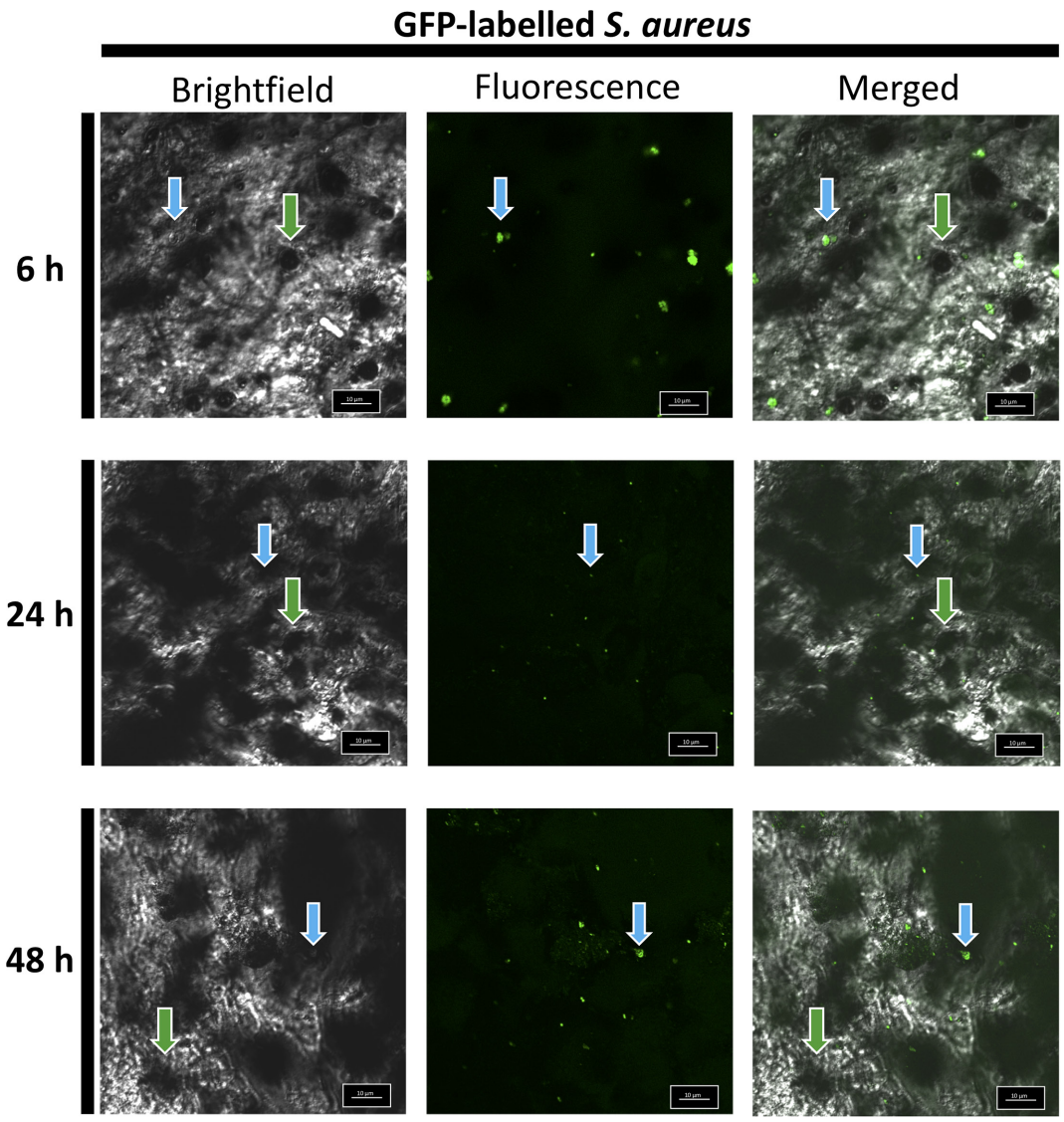

Fig. 4. Visualization of GFP-labelled *S. aureus* cells within bacterial nodules in *G. mellonella* larvae inoculated with 2×10^6 viable cells. Bacterial nodules were dissected from larvae infected with *S. aureus* for 6, 24 and 48 h and visualized using confocal microscopy. Brightfield images reveal the formation of melanized plaques (green arrow). Fluorescent microscopy revealed an abundance of *S. aureus* cells (blue arrows) within nodules at 6, 24 and 48 h post-infection (scale bar corresponds to 10 µm).

Alteration in hemocyte density and function in response to *S. aureus* infection

Inoculation of larvae with *S. aureus* (2×10^6 cells larva^{-1}) resulted in a spike in hemocyte density at 4 h $1.47\pm0.25\times10^6$ larva^{-1} (60 µl hemolymph), $P<0.05$] as compared to the control ($4.71\pm0.66\times10^5$). There was also an increase in hemocyte density at 6 h ($6.23\pm8.61\times10^5$, $P<0.05$) compared to the control ($2.81\pm0.15\times10^5$). Larvae infected with *S. aureus* for 24 ($6.65\pm1.66\times10^5$, $P<0.05$) and 72 h ($1.29\pm0.16\times10^6$, $P<0.05$) showed a significant increase in hemocyte density compared to the controls (Fig. 5).

Hemocytes from larvae that were treated with heat-killed *S. aureus* (2×10^6 20 µl^{-1}) for 24 h displayed an increased ability to kill yeast cells as compared to hemocytes from control larvae and larvae treated with *S. aureus* for 6 h. Hemocytes from larvae treated with *S. aureus* for 24 h reduced the viability of *C. albicans* to 3.49±0.69 % ($P<0.01$) at 60 min and 1.39±1.39 % ($P<0.05$) at 80 min compared to the controls at the same time points (60 min, 53.98±10.62 %; 80 min, 25.63±6.14 %) (Fig. 6).

Incubation of hemocytes with *S. aureus* (2 : 1 ratio) for 5 and 20 min indicated hemocyte lysis around *S. aureus* cells (white

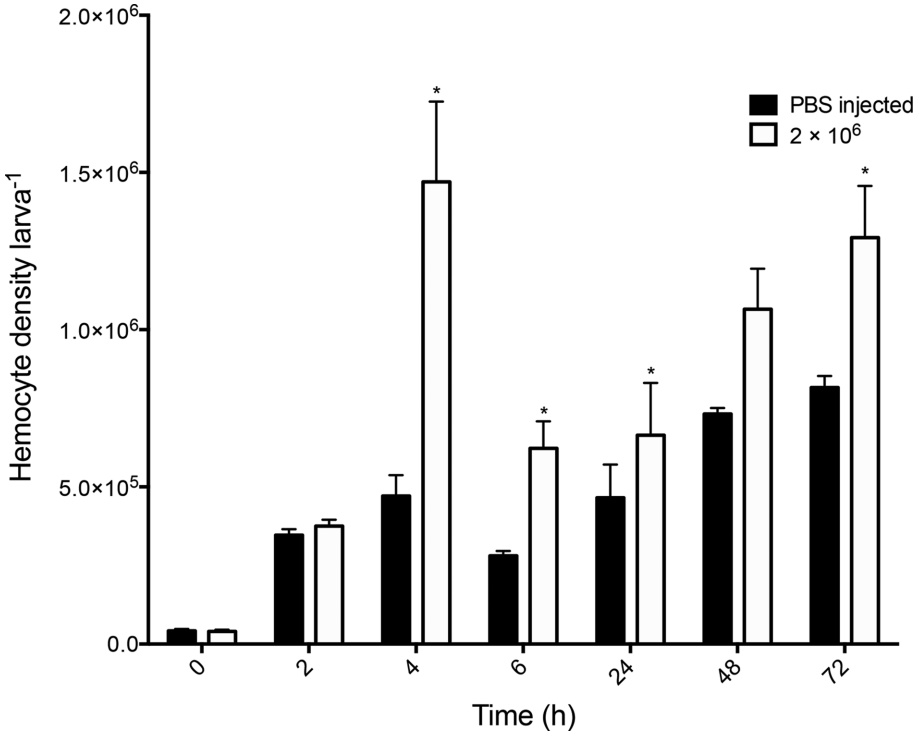

Fig. 5. Alteration in circulating hemocyte density following inoculation with viable *S. aureus* cells. *G. mellonella* larvae were inoculated with 20 µl *S. aureus* cells (2×10^6) or PBS and hemocytes were extracted and enumerated from 0 to 72 h post-inoculation. Statistical analysis was performed by comparing treatments to PBS-injected controls at respective time points (*P<0.05). All values are the mean ±SE of three independent experiments.

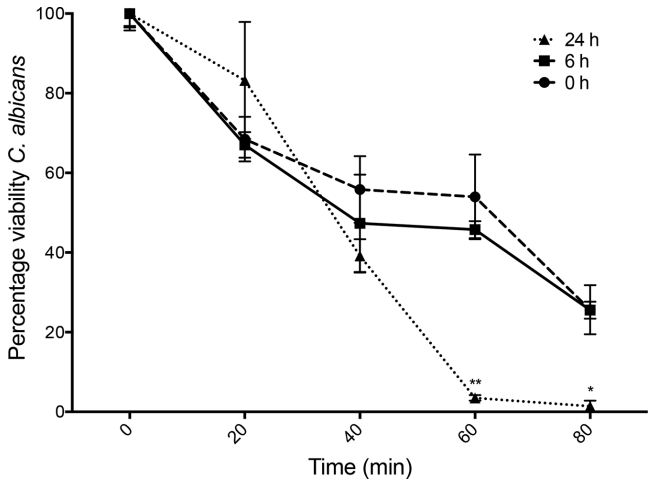

Fig. 6. Microbicidal activity of hemocytes extracted from *G. mellonella* larvae at 0, 6 and 24 h after inoculation with heat-killed *S. aureus* cells (2×10^6 larva^{-1}). Pre-opsonized *C. albicans* cells were incubated with hemocytes (2 : 1 ratio) for 80 min and aliquots were taken every 20 min, diluted and plated on YEPD agar plates (*P<0.05, **P<0.01). All values are the mean ±SE of three independent experiments.

arrows) (Figs 7 and S2). This process has been also reported elsewhere with fungal cells [18].

Humoral immune response of larvae *to S. aureus* infection

Quantitative proteomics was performed on hemocyte-free hemolymph (hemocytes were removed by centrifugation at 10 000 ***g*** for 10 min) from larvae infected with *S. aureus* (2×10^6 larva^{-1}) at 0, 6 and 24 h. In total, 331 proteins were identified consisting of 2121 peptides. Of these, 18 proteins for 6 vs 0 h and 33 proteins for 24 vs 0 h were found to be differentially abundant with a fold change >1.5. In total, 12 proteins were found to be exclusive to 6 and 24 h treatments. A principal component analysis (PCA) of the proteins present at all three time points indicated that there was a distinct difference between the proteomes at 0, 6 and 24 h (Fig. S3).

Proteins that showed increased abundance in the 6 h-infected larvae when compared to the uninfected control larvae included hypothetical protein (43-fold increase), gloverin (14 -old increase), gustatory receptor candidate 25 (10-fold increase), peptidoglycan-recognition protein-LB (9-fold increase), peptidoglycan recognition-like protein B (5-fold increase) and beta actin (4-fold increase) (Table 1). The

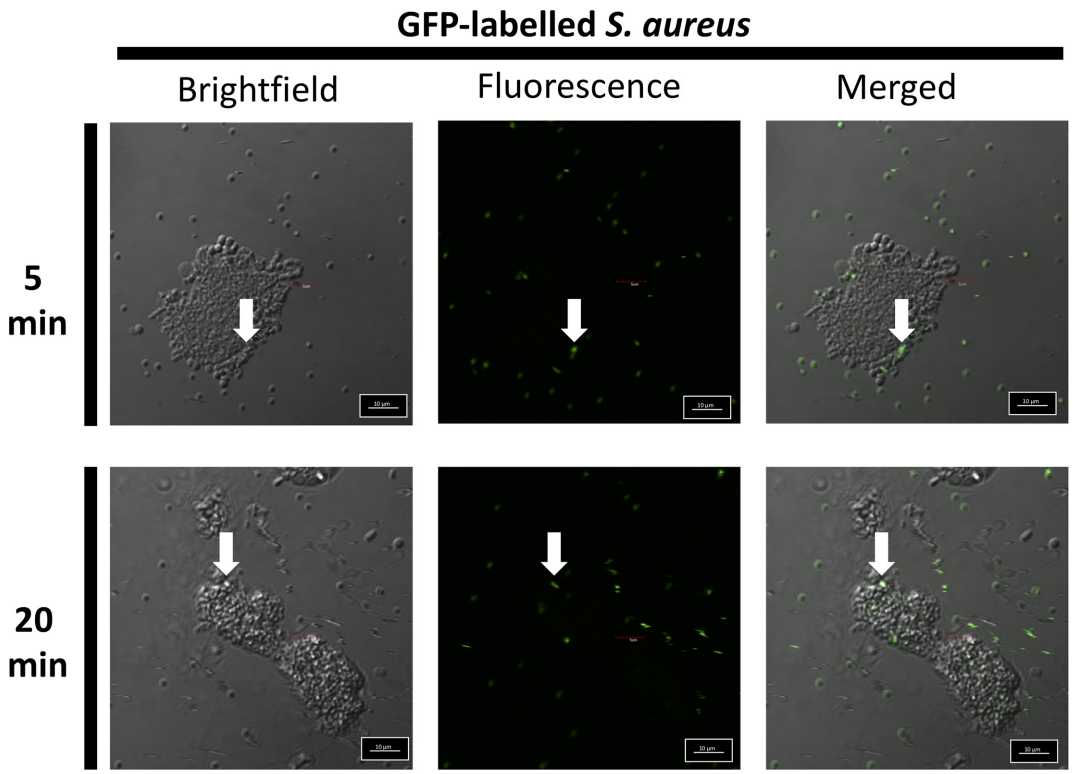

Fig. 7. Response of *ex vivo* hemocytes to *S. aureus*. Hemocytes were extracted from *G. mellonella* larvae washed three times with PBS and mixed for 5 and 20 min at a 1 : 1 ratio. Brightfield images of GFP-labelled *S. aureus* suggest the lysis of hemocytes around *S. aureus* cells (white arrows) (scale bar corresponds to 10 µm).

proteins that showed decreased abundance at 6 h compared to 0 h were alpha esterase 45 (1.6-fold decrease) and hypothetical protein (2-fold decrease) (Fig. 8). Proteins that showed increased abundance in the 24 h-infected larvae compared to 0 h included gloverin (86-fold increase), cecropin-D like peptide (79-fold increase), hypothetical protein (46-fold increase), cecropin-A (30-fold increase), gloverin-like protein (23-fold increase), lysozyme (18-fold increase), peptidoglycan recognition-like protein B (17-fold increase), peptidoglycan-recognition protein-LB (15-fold increase), inducible metalloproteinase inhibitor protein (10-fold increase) and hemolin (9-fold increase) (Table 2). The proteins that showed decreased abundance at 24 h compared to 0 h were cathepsin B-like cysteine proteinase (4-fold decrease), heat shock protein 25.4 precursor (3-fold decrease), hypothetical protein (2.7-fold decrease), serine proteinase (2.7-fold decrease) and hypothetical protein (2.3-fold decrease) (Fig. 8).

DISCUSSION

In recent years *G. mellonella* larvae, and other insect species, have been employed to assess the virulence of a range of bacterial species and produce results that correlate with those generated using mice [22, 52]. While *G. mellonella* larvae offer a number of advantages that overcome the drawbacks associated with mammalian testing and other model systems, there is now the opportunity to model bacterial infection processes in larvae and to characterize similarities with this process in mammals.

Infection with *S. aureus* dose-dependently decreased larval viability at 37 °C. In mice, an inoculum of 10^8 c.f.u. per mouse resulted in 50 % survival after 2 days and 0 % survival after 4 days [53]. Bacterial load peaked at 72 h and this is associated with a significant decrease in larval viability. In neutrophil-depleted mice, *S. aureus* can significantly proliferate within blood and skin samples [54].

At 6 h post-infection there were small nodules around the site of inoculation but no melanization of the cuticle. At 6 h *S. aureus* appeared in clumps, but by 24 h single cells were present within nodules and this occurred with extensive melanized nodule formation around the hemocoel of the larvae. By 48 h widespread melanization of insect hemolymph had occurred, possibly due to uncontrolled phenoloxidase activation due to an uncontrollable bacterial burden. A small number of nodules were produced as compared to infection by fungal pathogens and this may have been due to clumping of *S. aureus* cells.

Nodules produced in *G. mellonella* larvae during infection are similar in structure and function to the abscesses commonly found during *S. aureus* skin and soft tissue infection in

Table 1. Proteins which were considered statistically significant and differentially abundant (SSDA) in *G. mellonella larvae* hemolymph infected with *S. aureus* for 6 h as compared to 0 h (Red:increased in abundance,Green; decreased in abundance)

Protein name	No. of peptides	Sequence coverage (%)	Score	*P value*	Fold change
Gloverin	3	46.2	42.566	5.27E-05	20.06
Gustatory receptor	6	40.9	62.929	0.0002057	18.14
Uncharacterized protein	6	22.7	100.94	0.0115559	16.19
Serpin-4B	5	78.8	41.117	0.007772	6.63
Peptidoglycan-recognition protein-LB	3	72.4	39.312	0.024767	5.97
Peptidoglycan recognition-like protein B	13	34	296.93	0.0013876	5.41
Uncharacterized protein	3	19	75.959	0.0154921	4.76
Beta actin	9	52	261.97	0.0024351	4.61
AGAP011516-PA	5	14.5	38.671	0.0316638	3.99
Prophenol oxidase-activating enzyme 3	5	44.4	55.786	0.0316365	2.85
Protease inhibitor 1	15	37	169.5	0.0313505	2.56
Uncharacterized protein	3	21.2	183.66	0.0427484	2.1
Serine protease inhibitor dipetalogastin	3	15.5	40.032	0.0185339	1.98
Fructose-1,6-bisphosphatase	12	28	323.31	0.0083192	1.92
Arginine kinase	2	29.1	53.86	0.0300812	1.82
Putative hydroxypyruvate isomerase	10	71.1	224.42	0.0128579	1.68
Carboxylic ester hydrolase	11	31.5	103.82	0.0202315	1.63
Alpha-esterase 45	5	8.5	48.709	0.002778	−1.63

humans [55]. *S. aureus* produces several molecules that contribute to abscess formation and these recruit neutrophils and induce host cell lysis and the formation of the fibrin capsules that surround the abscesses [55]. Abscess formation is associated with a characteristic decrease in *S. aureus* c.f.u. load, but this may be associated with an increase within tissue [56]. This was also observed in this study as the total *S. aureus* c.f.u. decreased in larvae between 2 and 4 h. *S. aureus*

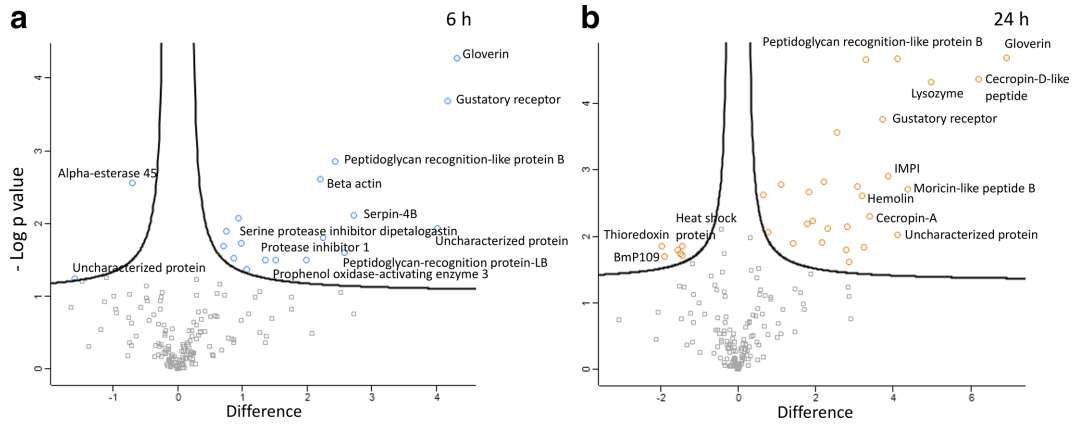

Fig. 8. Proteomic responses of *G. mellonella* larval hemolymph following infection by 2×10^6 *S. aureus* cells after 6 (a) and 24 h (b). Volcano plots represent protein intensity difference ($\log_2$ mean intensity difference) and significance in differences (log *P* value) based on a two-sided T-TEST. Proteins above the line are considered statistically significant (*P* value<0.05) and those to the right and left of the vertical lines indicate relative fold changes >1.5. Annotations are given for the most differentially abundant proteins identified in hemolymph from larvae infected with *S. aureus* for 6 and 24 h. These plots are based upon post-imputed data.

Table 2. Proteins which were considered statistically significant and differentially abundant in *G. mellonella larvae* hemolymph infected with *S. aureus* for 24 h as compared to 0 h (Red: increased in abundance, Green; decreased in abundance)

Protein name	No. of peptides	Sequence coverage (%)	Score	*P value*	Fold change
Gloverin	3	46.2	42.566	2.05E-05	121.69
Cecropin-D-like peptide	2	14.5	81.412	4.40E-05	73.7
Lysozyme	6	19.1	45.237	4.73E-05	31.38
Moricin-like peptide B	1	13.3	14.208	0.001982	20.81
Peptidoglycan recognition-like protein B	13	34	296.93	2.12E-05	17.35
Uncharacterized protein	6	22.7	100.94	0.009474	17.23
Inducible metalloproteinase inhibitor protein	7	35.1	99.811	0.001234	14.61
Gustatory receptor	6	40.9	62.929	0.000171	13.3
Cecropin-A (cecropin-C)	1	8.5	9.4615	0.005058	10.56
Uncharacterized protein	3	19	75.959	2.23E-05	9.88
Peptidoglycan-recognition protein-LB	3	72.4	39.312	0.014231	9.53
Hemolin	5	53.6	106.13	0.002471	9.23
Hemolin	16	51.5	323.31	0.001797	8.39
Putative defence protein Hdd11	6	34.2	53.851	0.024342	7.24
Serpin-4B	5	78.8	41.117	0.007182	7.03
Yellow-d	12	26.6	196.65	0.016128	6.96
Protease inhibitor 1	3	21.2	183.66	0.000272	5.81
Prophenol oxidase-activating enzyme 3	15	37	169.5	0.007552	4.97
Peptidoglycan recognition protein	11	56	313.13	0.0015	4.64
Chemosensory protein 7	4	21	181.63	0.012462	4.5
Gloverin	2	14.8	13.135	0.005864	3.83
Sulfhydryl oxidase 1	5	26.2	105.27	0.002125	3.54
Prophenoloxidase-activating protease I	2	57.7	21.028	0.006467	3.46
Serine protease inhibitor dipetalogastin	12	28	323.31	0.012544	2.68
Beta-1,3-glucan recognition protein	19	41.4	315.64	0.001665	2.16
Inducible serine protease inhibitor 2	3	9.8	111.22	0.00849	1.72
Hemolymph proteinase 16	10	38.2	146.66	0.0024	1.57
Serine proteinase	14	34	323.31	0.019384	−2.7
Uncharacterized protein	2	5.6	58.117	0.014143	−2.71
Cathepsin B-like cysteine proteinase	4	13.8	41.669	0.017993	−2.79
Heat shock protein 25.4	13	48	323.31	0.016116	−2.93
BmP109	7	23.4	60.397	0.019927	−3.72
Thioredoxin	3	13.6	35.124	0.014066	−3.94

invasion triggers predominantly neutrophils and macrophage infiltration and this is associated with residence of *S. aureus* within neutrophils. Within 72 h staphylococci are localized within abscesses at the centre of the lesions, enclosed by fibrin deposits and surrounded by layers of immune cells [56, 57].

Inoculation of larvae with 2×10^6 *S. aureus* cells resulted in a significant increase in the numbers of circulating hemocytes at 4 h, possibly due to the release of hemocytes usually attached to the linings of internal organs such as body fat [58]. There was also an increase in hemocyte density at 6 and 24 h post-infection and this was correlated with the replication of *S. aureus* cells within larvae. Interestingly, human neutrophils (which are analogous to insect hemocytes) are first recruited to the site of *S. aureus* infection and the accumulation of neutrophils is effective in *S. aureus* killing [59–61]. In *G. mellonella* larvae hemocytes can be differentiated into at least five types of cells, including prohemocytes (precursor cells), granulocytes, which are usually spherical with lobulated nuclei, and plasmatocytes (the most abundant cell type in the hemolymph), which are small round-shaped pseudopodia-producing cells with adherent properties, and engage in phagocytosis, encapsulation and nodulation processes [62–64]. In mice infected with 10^7 or 10^8 *S. aureus* cells, circulating granulocyte density peaked at 6 h and was higher in mice infected with the higher dose [53]. BALB/c mice infected with *S. aureus* (10^8) displayed a significant increase in neutrophil density before a spike in *S. aureus* proliferation was observed [65], and in this study hemocyte density peaked prior to accelerated *S. aureus* proliferation.

Hemocytes from larvae exposed to heat-killed *S. aureus* for 24 h were more microbicidal than control hemocytes and hemocytes from larvae exposed for 6 h, indicating the possible appearance of a specific cell type (e.g. granulocyte) with superior killing ability. Interactions between *S. aureus* and larval hemocytes resulted in hemocyte degranulation and lysis, and this is the early stage of nodule formation around the microbial invader (Fig. 7), which is also observed with fungal cells [18].

Proteomic analysis of larval hemolymph at 6 and 24 h post-infection with *S. aureus* revealed a range of proteins that are involved in regulation of the immune response, defence against bacterial infection and nodule formation. There was also an increase in a range of opsonins, such as peptidoglycan-recognition protein-LB and peptidoglycan recognition-like protein B, at 6 h post-infection, which play an important role in bacterial cell identification and recognition by circulating immune cells [66]. Components of the prophenoloxidase cascade (prophenoloxidase-activating enzyme 3) were also increased in abundance in the proteome of 6 h *S. aureus*-infected hemolymph. The phenoloxidase cascade is analogous to the mammalian complement cascade in terms of protein structure, function and mode of action [67, 68]. *S. aureus* interacts with and evades the complement cascade at many levels [69]. At 6 h post-infection the antimicrobial protein showing the greatest increase in abundance was gloverin. Gloverin is a glycine-rich, heat-stable antibacterial protein believed to bind lipopolysaccharides (LPS) and it was previously demonstrated that *E. coli* induced its expression in *Bombyx mori* [70].

By 24 h post-infection a range of antimicrobial peptides (AMPs), such as gloverin, cecropin-D-like peptide, lysozyme and moricin-like peptide B, showed increased abundance. The AMP family cecropin were first isolated from *Hyalophora cecropia* and demonstrate antibacterial activity against multidrug-resistant *Acinetobacter baumannii* and *P. aeruginosa* and display immunomodulatory effects on macrophages [71]. Cecropin A displays antimicrobial activity against *S. aureus* [72], but protoplasts are resistant to cecropin B [73]. Lysozyme was also increased in abundance in response to *S. aureus* infection and cleaves the β–1,4 glycosidic bonds between N-acetylmuramic acid and N-acetylglucosamine of bacterial peptidoglycan and induces bacterial lysis. However, many *S. aureus* strains display intrinsic resistance to lysozyme and its activity acts in synergy with other AMPs and the cellular immune response [74, 75]. Moricins are secreted propeptides that are are activated via proteolysis and increase the permeability of bacterial membranes [76]. *B. mori* moricin is active against *S. aureus*, targets the membrane and is induced by bacterial infection [76]. A range of human AMPs are essential in the defence against *Staphylococcus* infection. Pathogenic *S. aureus* primarily induce human β-defensin (hBD) 1 and hBD3. LL-37 is expressed on the skin and is an important defence against *S. aureus* invasion, displaying important bactericidal activity against *S. aureus* [77]. *S. aureus* induces the expression of hBD3 and hCAP-18, while methicillin-resistant *S. aureus* is more resistant to AMPs than its methicillin-susceptible counterpart [78].

A number of proteins involved in nodule formation in *G. mellonella* larvae were also increased in abundance, such as putative defence protein hdd11 and hemolin. Hdd11 was increased in hemolymph at 24 h post-infection with *S. aureus* and has been found to be increased in *Hyphantria cunea* during bacterial infection and shares homology with noduler from *Antheraea mylitta* [79, 80]. Noduler shares a reeler domain with Hdd11 and binds both insect hemocytes and bacterial LPS, is enriched within nodules and is important during the nodulation response [81]. The immunoglobulin superfamily member hemolin was induced by *Candida* challenge and has been shown to act as a pattern recognition receptor in insects [82, 83]. Hdd11 and hemolin have also showed increased abundance in larvae infected with *Aspergillus fumigatus* and *C. albicans*. Fungal infection of larvae also results in a more dramatic increase in AMPs, proteins associated with cellular stress, invasion of fungal hyphae and a range of β-glucan binding proteins [18, 19].

The results presented here detail the cellular and humoral responses of larvae to *S. aureus* during the development of disseminated disease. These results show similarities to the interaction of *S. aureus* with the immune response in mammals (i.e. rapid bacterial proliferation, nodule formation, alteration in immune cell numbers and increased antimicrobial peptide abundance). Studying the development

of *S. aureus* infection in larvae may give novel insights into the pathogen–host interactions that could improve our understanding of this disease process in mammals. These similarities may also be used to study the efficacy and interaction of novel antibiotics with *S. aureus* in combination with the host immune response, while overcoming the disadvantages associated with using mice in early-stage drug development.

Funding information
G. S. is the recipient of a Maynooth University Doctoral studentship. The Q-exactive mass spectrometer was funded under the SFI Research Infrastructure Call 2012 [grant number: 12/RI/2346 (3)].

Author contributions
G. S. and K. K. designed the experiments. G. S. and A. D. performed the experiments and analysed the results. G. S. and K. K. wrote the manuscript. All authors have read and approved the manuscript.

Conflicts of interest
The authors declare that there are no conflicts of interest.

References

1. Otto M. Staphylococcal biofilms. *Curr Top Microbiol Immunol* 2008;322:207–228.
2. Brown AF, Leech JM, Rogers TR, McLoughlin RM. *Staphylococcus aureus* colonization: modulation of host immune response and impact on human vaccine design. *Front Immunol* 2014;8:4.
3. Tong SYC, Davis JS, Eichenberger E, Holland TL, Fowler VG. *Staphylococcus aureus* infections: epidemiology, pathophysiology, clinical manifestations, and management. *Clin Microbiol Rev* 2015;28:603–661.
4. Lowy FD. *Staphylococcus aureus* infections. *N Engl J Med* 1998;339:520–532.
5. Bhakdi S, Tranum-Jensen J. Alpha-toxin of *Staphylococcus aureus*. *Microbiol Rev* 1991;55:733–751.
6. Spaulding AR, Salgado-Pabón W, Kohler PL, Horswill AR, Leung DYM *et al*. Staphylococcal and streptococcal superantigen exotoxins. *Clin Microbiol Rev* 2013;26:422–447.
7. Burman JD, Leung E, Atkins KL, O'Seaghdha MN, Lango L *et al*. Interaction of human complement with Sbi, a staphylococcal immunoglobulin-binding protein: indications of a novel mechanism of complement evasion by *Staphylococcus aureus*. *J Biol Chem* 2008;283:17579–17593.
8. Jongerius I, Köhl J, Pandey MK, Ruyken M, van Kessel KPM *et al*. Staphylococcal complement evasion by various convertase-blocking molecules. *J Exp Med* 2007;204:2461–2471.
9. Moreillon P, Entenza JM, Francioli P, McDevitt D, Foster TJ *et al*. Role of *Staphylococcus aureus* coagulase and clumping factor in pathogenesis of experimental endocarditis. *Infect Immun* 1995;63:4738–4743.
10. Hartleib RJ, Köhler N, Dickinson RB, Chhatwal GS, Sixma JJ *et al*. Protein A is the von Willebrand factor binding protein on *Staphylococcus aureus*. *Blood* 2000;96:2149–2156.
11. Shinji H, Yosizawa Y, Tajima A, Iwase T, Sugimoto S *et al*. Role of fibronectin-binding proteins A and B *in in* vitro cellular infections and *in* vivo septic infections by *Staphylococcus aureus*. *Infect Immun* 2011;79:2215–2223.
12. Bunce C, Wheeler L, Reed G, Musser J, Barg N. Murine model of cutaneous infection with gram-positive cocci. *Infect Immun* 1992;60:2636–2640.
13. Weiss WJ, Lenoy E, Murphy T, Tardio LA, Burgio P. Effect of srtA and srtB gene expression on the virulence of *Staphylococcus aureus* in animal models of infection. *J Antimicrob Chemother* 2004;53:480–486.
14. Tarkowski A, Collins LV, Gjertsson I, Hultgren OH, Jonsson IM *et al*. Model systems: modeling human staphylococcal arthritis and sepsis in the mouse. *Trends Microbiol* 2001;9:321–326.
15. Santoro J, Levison ME. Rat model of experimental endocarditis. *Infect Immun* 1978;19:915–918.
16. Prajsnar TK, Cunliffe VT, Foster SJ, Renshaw SA. A novel vertebrate model of *Staphylococcus aureus* infection reveals phagocyte-dependent resistance of zebrafish to non-host specialized pathogens. *Cell Microbiol* 2008;10:2312–2325.
17. Sifri CD, Begun J, Ausubel FM, Calderwood SB. Caenorhabditis elegans as a model host for *Staphylococcus aureus* pathogenesis. *Infect Immun* 2003;71:2208–2217.
18. Sheehan G, Clarke G, Kavanagh K. Characterisation of the cellular and proteomic response of *Galleria mellonella* larvae to the development of invasive aspergillosis. *BMC Microbiol* 2018;18:63.
19. Sheehan G, Kavanagh K. Analysis of the early cellular and humoral responses of *Galleria mellonella* larvae to infection by *Candida albicans*. *Virulence* 2018;9:163–172.
20. Mukherjee K, Hain T, Fischer R, Chakraborty T, Vilcinskas A. Brain infection and activation of neuronal repair mechanisms by the human pathogen *Listeria monocytogenes* in the lepidopteran model host *Galleria mellonella*. *Virulence* 2013;4:324–332.
21. Sheehan G, Garvey A, Croke M, Kavanagh K. Innate humoral immune defences in mammals and insects: The same, with differences ? *Virulence* 2018;9:1625–1639.
22. Jander G, Rahme LG, Ausubel FM. Positive correlation between virulence of *Pseudomonas aeruginosa* mutants in mice and insects. *J Bacteriol* 2000;182:3843–3845.
23. Brennan M, Thomas DY, Whiteway M, Kavanagh K. Correlation between virulence of *Candida albicans* mutants in mice and *Galleria mellonella* larvae. *FEMS Immunol Med Microbiol* 2002;34:153–157.
24. Kavanagh K, Sheehan G. The use of *Galleria mellonella* larvae to identify novel antimicrobial agents against fungal species of medical interest. *JoF* 2018;4:113.
25. Tsai CJ, Loh JM, Proft T, Jia C, Tsai -Yun, Mei J, Loh S. *Galleria mellonella* infection models for the study of bacterial diseases and for antimicrobial drug testing. *Virulence* 2016;7:214–229.
26. Allegra E, Titball RW, Carter J, Champion OL. *Galleria mellonella* larvae allow the discrimination of toxic and non-toxic chemicals. *Chemosphere* 2018;198:469–472.
27. Olsen RJ, Watkins ME, Cantu CC, Beres SB, Musser JM. Virulence of serotype M3 group A *Streptococcus* strains in wax worms (*Galleria mellonella* larvae). *Virulence* 2011;2:111–119.
28. Evans BA, Rozen DE. A *Streptococcus pneumoniae* infection model in larvae of the wax moth *Galleria mellonella*. *Eur J Clin Microbiol Infect Dis* 2012;31:2653–2660.
29. La Rosa SL, Leanti La Rosa S, Casey PG, Hill C, Diep DB *et al*. *In* vivo assessment of growth and virulence gene expression during commensal and pathogenic lifestyles of *luxABCDE*-tagged Enterococcus faecalis strains *in* murine gastrointestinal and intravenous infection models. *Appl Environ Microbiol* 2013;79:3986–3997.
30. La Rosa SL, Diep DB, Nes IF, Brede DA. Construction and application of a *luxABCDE* reporter system for real-time monitoring of *Enterococcus faecalis* gene expression and growth. *Appl Environ Microbiol* 2012;78:7003–7011.
31. Junior C, Fuchs J, Sabino BB, Junqueira CP, Jorge JC *et al*. Photodynamic and antibiotic therapy impair the pathogenesis of *Enterococcus faecium* in a whole animal insect model. *PLoS One* 2013;8.
32. Lebreton F, Le Bras F, Reffuveille F, Ladjouzi R, Giard JC *et al*. *Galleria mellonella* as aModel for studying *Enterococcus faecium* host persistence. *J Mol Microbiol Biotechnol* 2012;21:191–196.
33. Desbois AP, Coote PJ. Wax moth larva (Galleria mellonella): an in vivo model for assessing the efficacy of antistaphylococcal agents. *J Antimicrob Chemother* 2011;66:1785–1790.
34. Peleg AY, Monga D, Pillai S, Mylonakis E, Moellering RC Jr *et al*. Reduced susceptibility to vancomycin influences pathogenicity in *Staphylococcus aureus* infection. *J Infect Dis* 2009;199:532–536.

35. Mukherjee K, Altincicek B, Hain T, Domann E, Vilcinskas A *et al*. *Galleria mellonella* as a model system for studying *Listeria pathogenesis*. *Appl Environ Microbiol* 2010;76:310–317.
36. Joyce SA, Gahan CGM. Molecular pathogenesis of *Listeria monocytogenes* in the alternative model host *Galleria mellonella*. *Microbiology* 2010;156:3456–3468.
37. Andrejko M, Cytryńska M, Jakubowicz T. Apolipophorin III is a substrate for protease IV from *Pseudomonas aeruginosa*. *FEMS Microbiol Lett* 2005;243:331–337.
38. Andrejko M, Mizerska-Dudka M. Elastase B of *Pseudomonas aeruginosa* stimulates the humoral immune response in the greater wax moth, *Galleria mellonella*. *J Invertebr Pathol* 2011;107:16–26.
39. Riza NA, Madamopoulos N. All-fiber connectorized fiber-optic delay module using 3-D polarization optics. *Conf Proc - Lasers Electro-Optics Soc Annu Meet* 1997;2:472–473.
40. Ciesielczuk H, Betts J, Phee L, Doumith M, Hope R *et al*. Comparative virulence of urinary and bloodstream isolates of extra-intestinal pathogenic *Escherichia coli* in a *Galleria mellonella* model. *Virulence* 2015;6:145–151.
41. Wand ME, McCowen JWI, Nugent PG, Sutton JM. Complex interactions of *Klebsiella pneumoniae* with the host immune system in a *Galleria mellonella* infection model. *J Med Microbiol* 2013;62:1790–1798.
42. Diago-Navarro E, Chen L, Passet V, Burack S, Ulacia-Hernando A *et al*. Carbapenem-resistant *Klebsiella pneumoniae* exhibit variability in capsular polysaccharide and capsule associated virulence traits. *J Infect Dis* 2014;210:803–813.
43. Harding CR, Stoneham CA, Schuelein R, Newton H, Oates CV *et al*. The Dot/Icm effector SdhA is necessary for virulence of *Legionella pneumophila* in *Galleria mellonella* and A/J mice. *Infect Immun* 2013;81:2598–2605.
44. Harding CR, Schroeder GN, Reynolds S, Kosta A, Collins JW *et al*. *Legionella pneumophila* pathogenesis in the *Galleria mellonella* infection model. *Infect Immun* 2012;80:2780–2790.
45. Jacobs AC, Thompson MG, Black CC, Kessler JL, Clark LP *et al*. AB5075, a highly virulent isolate of *Acinetobacter baumannii*, as a model strain for the evaluation of pathogenesis and antimicrobial treatments. *MBio* 2014;5.
46. Peleg AY, Jara S, Monga D, Eliopoulos GM, Moellering RC *et al*. *Galleria mellonella* as a model system to study *Acinetobacter baumannii* pathogenesis and therapeutics. *Antimicrob Agents Chemother* 2009;53:2605–2609.
47. Geoghegan JA, Corrigan RM, Gruszka DT, Speziale P, O'Gara JP *et al*. Role of surface protein SasG in biofilm formation by *Staphylococcus aureus*. *J Bacteriol* 2010;192:5663–5673.
48. Silva LN, Da Hora GCA, Soares TA, Bojer MS, Ingmer H *et al*. Myricetin protects *Galleria mellonella* against *Staphylococcus aureus* infection and inhibits multiple virulence factors. *Sci Rep* 2017;7.
49. Cox J, Neuhauser N, Michalski A, Scheltema RA, Olsen JV *et al*. Andromeda: a peptide search engine integrated into the MaxQuant environment. *J Proteome Res* 2011;10:1794–1805.
50. Vogel H, Altincicek B, Glöckner G, Vilcinskas A. A comprehensive transcriptome and immune-gene repertoire of the lepidopteran model host *Galleria mellonella*. *BMC Genomics* 2011;12:308.
51. Côté RG, Griss J, Dianes JA, Wang R, Wright JC *et al*. The proteomics identification (pride) converter 2 framework: an improved suite of tools to facilitate data submission to the pride database and the ProteomeXchange Consortium. *Mol Cell Proteomics* 2012;11:1682–1689.
52. Gaddy JA, Arivett BA, McConnell MJ, López-Rojas R, Pachón J *et al*. Role of acinetobactin-Mediated iron acquisition functions in the interaction of Acinetobacter baumannii strain ATCC 19606T with human lung epithelial cells, *Galleria mellonella* caterpillars, and mice. *Infect Immun* 2012;80:1015–1024.
53. Capparelli R, Parlato M, Borriello G, Salvatore P, Iannelli D. Experimental phage therapy against *Staphylococcus aureus* in mice. *Antimicrob Agents Chemother* 2007;51:2765–2773.
54. Mölne L, Verdrengh M, Tarkowski A. Role of neutrophil leukocytes in cutaneous infection caused by *Staphylococcus aureus*. *Infect Immun* 2000;68:6162–6167.
55. Kobayashi SD, Malachowa N, DeLeo FR. Pathogenesis of Staphylococcus aureus abscesses. *Am J Pathol* 2015;185:1518–1527.
56. Cheng AG, Kim HK, Burts ML, Krausz T, Schneewind O *et al*. Genetic requirements for *Staphylococcus aureus* abscess formation and persistence in host tissues. *FASEB J* 2009;23:3393–3404.
57. Thomer L, Schneewind O, Missiakas D. Pathogenesis of *Staphylococcus aureus* bloodstream infections. *Annu Rev Pathol Mech Dis* 2016;11:343–364.
58. Ratcliffe NA. Invertebrate immunity-a primer for the non-specialist. *Immunol Lett* 1985;10:253–270.
59. Guerra FE, Borgogna TR, Patel DM, Sward EW, Voyich JM. Epic immune battles of history: neutrophils vs. *Staphylococcus aureus*. *Front Cell Infect Microbiol* 2017;7:286.
60. Li Y, Karlin A, Loike JD, Silverstein SC. A critical concentration of neutrophils is required for effective bacterial killing in suspension. *Proc Natl Acad Sci U S A* 2002;99:8289–8294.
61. Robertson CM, Perrone EE, McConnell KW, Dunne WM, Boody B *et al*. Neutrophil depletion causes a fatal defect in murine pulmonary *Staphylococcus aureus* clearance. *J Surg Res* 2008;150:278–285.
62. Neuwirth M. The structure of the hemocytes of *Galleria mellonella* (Lepidoptera). *J Morphol* 1973;139:105–123.
63. Price CD, Ratcliffe NA. A reappraisal of insect haemocyte classification by the examination of blood from fifteen insect orders. *Zeitschrift für Zellforsch. und mikroskopische Anat* 1974;147:537–549.
64. Strand MR. Insect hemocytes and their role in immunity. *Insect Immunol* 2008;32:25–47.
65. de Oliveira THC, Amorin AT, Rezende IS, Santos Barbosa M, Martins HB, Marques LM *et al*. Sepsis induced by *Staphylococcus aureus*: participation of biomarkers in a murine model. *Med Sci Monit* 2015;21:345–355.
66. Dziarski R. Peptidoglycan recognition proteins (PGRPs). *Mol Immunol* 2004;40:877–886.
67. Clow LA, Raftos DA, Gross PS, Smith LC. The sea urchin complement homologue, SPC3, functions as an opsonin. *J Exp Biol* 2004;207:2147–2155.
68. Söderhäll K, Cerenius L. Role of the prophenoloxidase-activating system in invertebrate immunity. *Curr Opin Immunol* 1998;10:23–28.
69. Lee LYL, Höök M, Haviland D, Wetsel RA, Yonter EO *et al*. Inhibition of complement activation by a secreted *Staphylococcus aureus* protein. *J Infect Dis* 2004;190:571–579.
70. Yi HY, Deng XJ, Yang WY, Zhou CZ, Cao Y *et al*. Gloverins of the silkworm Bombyx mori: structural and binding properties and activities. *Insect Biochem Mol Biol* 2013;43:612–625.
71. Yun J, Lee DG. Cecropin A-induced apoptosis is regulated by ion balance and glutathione antioxidant system in *Candida albicans*. *IUBMB Life* 2016;68:652–662.
72. Lee E, Jeong K-W, Lee J, Shin A, Kim J-K *et al*. Structure-activity relationships of cecropin-like peptides and their interactions with phospholipid membrane. *BMB Rep* 2013;46:282–287.
73. Moore AJ, Beazley WD, Bibby MC, Devine DA. Antimicrobial activity of cecropins. *J Antimicrob Chemother* 1996;37:1077–1089.
74. Bera A, Herbert S, Jakob A, Vollmer W, Götz F. Why are pathogenic staphylococci so lysozyme resistant? the peptidoglycan O-acetyltransferase OatA is the major determinant for lysozyme resistance of *Staphylococcus aureus*. *Mol Microbiol* 2005;55:778–787.
75. Chen X, Niyonsaba F, Ushio H, Okuda D, Nagaoka I *et al*. Synergistic effect of antibacterial agents human β-defensins, cathelicidin LL-37 and lysozyme against *Staphylococcus aureus* and *Escherichia coli*. *J Dermatol Sci* 2005;40:123–132.
76. Hara S, Yamakawa M. Moricin, a novel type of antibacterial peptide isolated from the silkworm, Bombyx mori. *J Biol Chem* 1995;270:29923–29927.

77. Ommori R, Ouji N, Mizuno F, Kita E, Ikada Y *et al*. Selective induction of antimicrobial peptides from keratinocytes by staphylococcal bacteria. *Microb Pathog* 2013;56:35–39.
78. Midorikawa K, Ouhara K, Komatsuzawa H, Kawai T, Yamada S *et al*. *Staphylococcus aureus* susceptibility to innate antimicrobial peptides, beta-defensins and CAP18, expressed by human keratinocytes. *Infect Immun* 2003;71:3730–3739.
79. Woon Shin S, Park SS, Park DS, Gwang Kim M, Brey PT *et al*. Isolation and characterization of immune-related genes from the fall webworm, Hyphantria cunea, using PCR-based differential display and subtractive cloning. *Insect Biochem Mol Biol* 1998;28:827–837.
80. Sarauer BL, Gillott C, Hegedus D. Characterization of an intestinal mucin from the peritrophic matrix of the diamondback moth, *Plutella xylostella*. *Insect Mol Biol* 2003;12:333–343.
81. Gandhe AS, John SH, Nagaraju J. Noduler, a novel immune up-regulated protein mediates nodulation response in insects. *J Immunol* 2007;179:6943–6951.
82. Browne N, Surlis C, Maher A, Gallagher C, Carolan JC *et al*. Prolonged pre-incubation increases the susceptibility of *Galleria mellonella* larvae to bacterial and fungal infection. *Virulence* 2015;6:458–465.
83. Yu XQ, Kanost MR. Binding of hemolin to bacterial lipopolysaccharide and lipoteichoic acid. An immunoglobulin superfamily member from insects as a pattern-recognition receptor. *Eur J Biochem* 2002;269:1827–1834.

Edited by: J. Stülke and P. Serror